Ena/VASP as possible antimetastatic target addressed by structure-optimized ProM scaffolds

M. Barone[1], R. Opitz[1], M. Müller[1], H.-G. Schmalz[2], R. Kühne[1]

[1] Leibniz-Institut für Molekulare Pharmakologie (FMP), Robert-Rössle-Str. 10, 13125 Berlin
[2] Universität zu Köln, Institut für Organische Chemie, Greinstr. 4, 50939 Cologne

The lack of metastasis-related targets

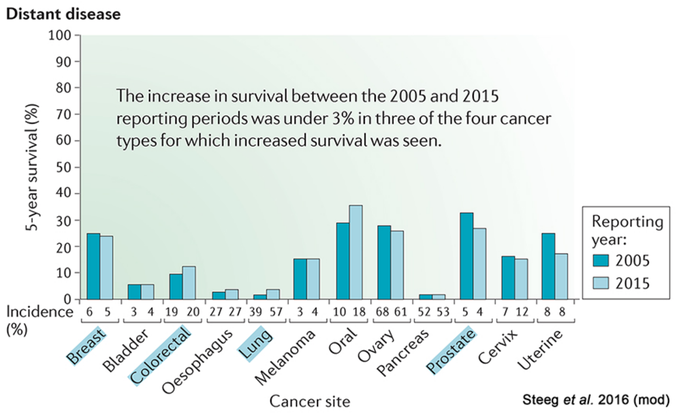

Tumor metastasis is the leading cause of mortality among cancer patients. If diagnosed with distant metastases, fewer than 20% of patients survive the next 5 years. Current approaches to metastatic disease are not improving satisfactorily. Hence, there is an urgent need for new approaches to address additional cancer metastasis-related targets

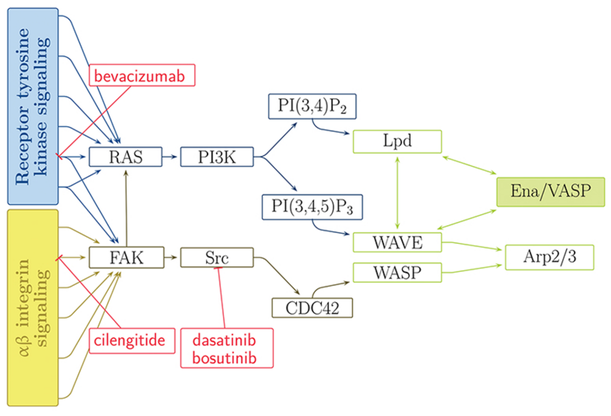

Ena/VASP proteins are elongation factors of F-actin at the very end of converging receptor kinase signaling (blue) and integrin (yellow) pathways. Antimetastatic drugs (red) inhibit druggable kinases signaling towards the actin interactome (green) which is governed by so-far undruggable protein-protein interactions.

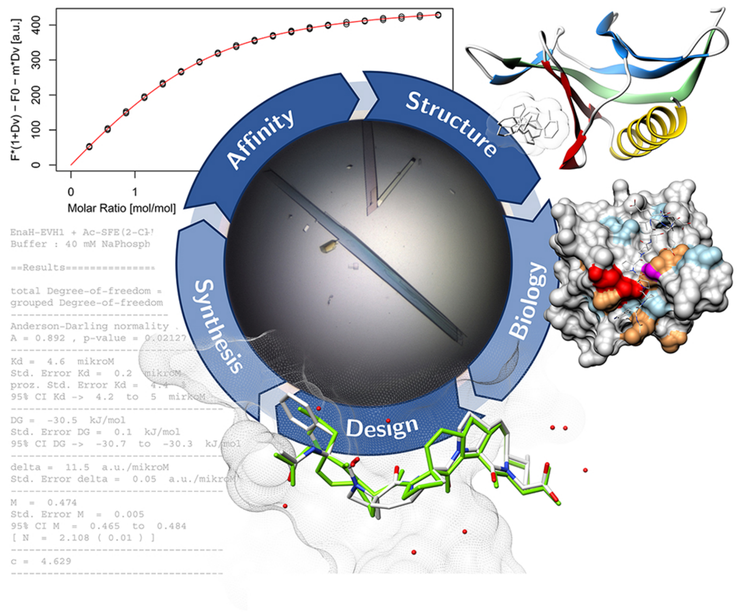

In a novel *in silico* designed approach, we used secondary structure mimetics to address the highly challenging proline-mediated protein-protein interaction of Ena/VASP.
Recently, we published an initial inhibitor that reduces breast cancer invasion in a Matrigel Boyden chamber assay by 80%.
On this poster, we present the combined biophysical analysis and high-resolution crystal structures as part of the iterative and interdisciplinary drug design cycle. The presented structure-based optimization is based on 19, partly deposited, complex structures that boosted the affinity more than 20-fold against a flat binding epitope. Cellular results and ongoing *in vivo* experiments are not shown.

The parent inhibitor

2-chloro-*L*-phenylalanine (2-Cl-Phe) and the combination of two di-proline-mimicking ProM scaffolds mimic core motif of the high-affinity, ActA-derived peptide **wt**. The affinity boost by these modifications allowed to shorten ligand **2** to the pentamer (**2a**). Masking the C-terminus with ethanol ester (OEt) rendered **2b** cell-membrane-permeable. However, the moderate affinity of **2b** will restrict the validation *in vivo*. Crystal structure of ENAH EVH1 in complex with **2a** (PDB code 4MY6, 1.7 Å resolution limit) and ^{1}H-^{15}N-HSQC experiments reveal that ProM scaffolds successfully mimic the proline-rich core motif. In structure-guided drug development effort, we sought to boost the affinity of **2b.**

Ligand composition		$K_{d,FT}$ [μM]	ΔG [kJ/mol]	$\Delta\Delta G$ [kJ/mol]
wt	Ac–SFEFPPPPTEDEL–NH_2	13.0 (0.6)	–27.9 (0.1)	(ref)
2	Ac–SFE[2-Cl-Phe][ProM-2][ProM-1]TEDEL–NH_2	0.15 (0.02)	–38.9 (0.2)	–8.1 (0.3)
2a	Ac–[2-Cl-Phe][ProM-2][ProM-1]–OH	2.3 (0.2)	–32.2 (0.2)	–4.3 (0.2)
2b	Ac–[2-Cl-Phe][ProM-2][ProM-1]–OEt	4.1 (0.3)	–30.8 (0.2)	–2.9 (0.2)

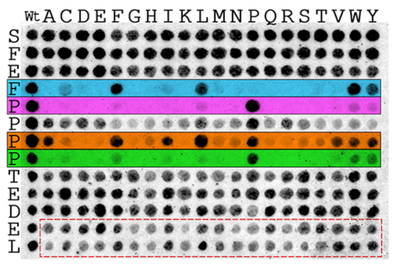

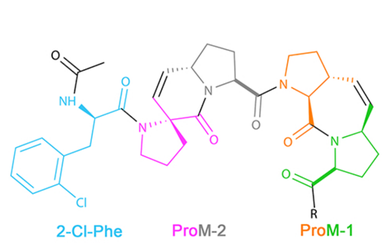

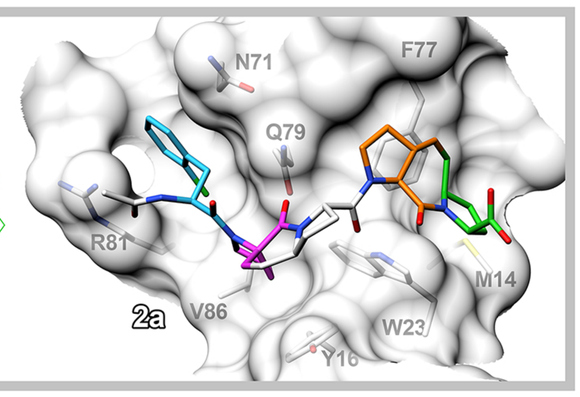

Optimization within the binding groove

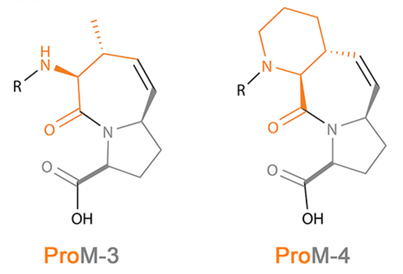

SPOT array substitution shows that Ena/VASP EVH1 accepts aliphatic residues instead of the third proline (orange). Two *in silico* designed scaffolds were synthesized, mimicking Xaa-*trans*-Pro. Unsubstituted amide backbone (ProM-3) results in a significant loss of affinity as EVH1 domains work with strict discriminatory mechanism for prolines. Intact backbone substitution by piperidine moiety (ProM-4) binds not significantly worse than reference inhibitor **2a** (95% confidence intervals 1.9-2.7 and 2.6-3.7 μM).
Superpositions with inhibitor **2a** reveal that both compositions **3a** and **4a** bound canonically to ENAH EVH1 (PDB codes 5NBF and 5NCF, high resolution limits 1.15 and 1.4 Å).

Ligand composition		$K_{d,FT}$ [μM]	ΔG [kJ/mol]	$\Delta\Delta G$ [kJ/mol]
2a	Ac–[2-Cl-Phe][ProM-2][ProM-1]–OH	2.3 (0.2)	–32.2 (0.2)	(ref)
3a	Ac–[2-Cl-Phe][ProM-2][ProM-3]–OH	9.7 (0.8)	–28.6 (0.2)	+3.6 (0.3)
4a	Ac–[2-Cl-Phe][ProM-2][ProM-4]–OH	3.0 (0.3)	–31.5 (0.2)	–0.7 (0.3)

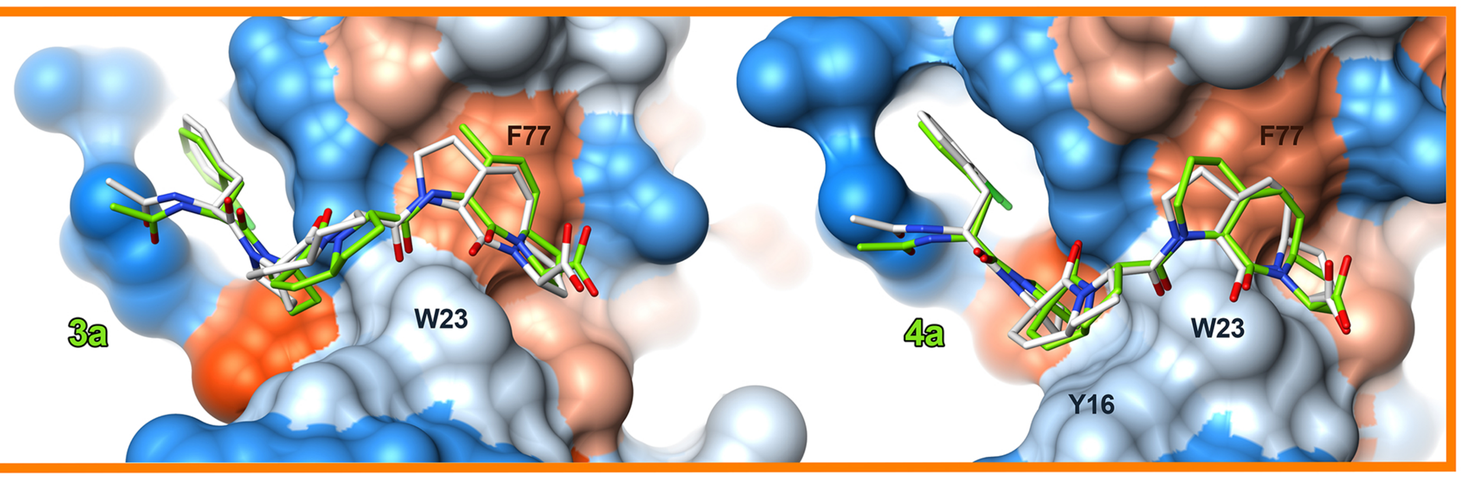

Finding epitopes beyond the binding groove

The flanking residues of chimera **2** provide 8 kJ/mol not accessible for inhibitor **2b**. Separate elongation (**2c,2d**) reveals that TEDEL affects affinity stronger than SFE. Glu-Leu is discussed as a second epitope whose truncation results in 5.5-fold reduced affinity on VASP EVH1 (Ball *et al.*). For the first time, we resolved the binding mode of these residues with high resolution limits up to 1.20 Å (PDB codes 5NC2, 5NC7, 5ND0) and found that TEDEL adopts helical loop. Only terminal Glu-Leu contact ENAH EVH1 with a mixture of polar and hydrophobic interactions. Mutation of Glu-Leu to Asp (**0b**) or Ala (**0c**) lost three-fold affinity. We therefore adressed both interaction sites with new ProM scaffolds.

Ligand composition		$K_{d,FT}$ [μM]	ΔG [kJ/mol]	$\Delta\Delta G$ [kJ/mol]
2b	Ac–[2-Cl-Phe][ProM-2][ProM-1]–OEt	4.1 (0.3)	–30.8 (0.3)	(ref)
2	Ac–SFE[2-Cl-Phe][ProM-2][ProM-1]TEDEL–NH_2	0.15 (0.02)	–38.9 (0.2)	–8.1 (0.3)
2c	Ac–[2-Cl-Phe][ProM-2][ProM-1]TEDEL–NH_2	0.33 (0.04)	–37.0 (0.3)	–6.2 (0.4)
2d	Ac–SFE[2-Cl-Phe][ProM-2][ProM-1]–OEt	2.9 (0.2)	–31.6 (0.1)	–0.8 (0.2)
0a	Ac–[2-Cl-Phe]PPPPTEDEL–NH_2	1.25 (0.04)	–33.7 (0.07)	(ref)
0b	Ac–[2-Cl-Phe]PPPPTEDDL–NH_2	3.8 (0.2)	–30.9 (0.01)	+2.8 (0.1)
0c	Ac–[2-Cl-Phe]PPPPTEDEA–NH_2	3.5 (0.1)	–31.2 (0.1)	+2.3 (0.1)

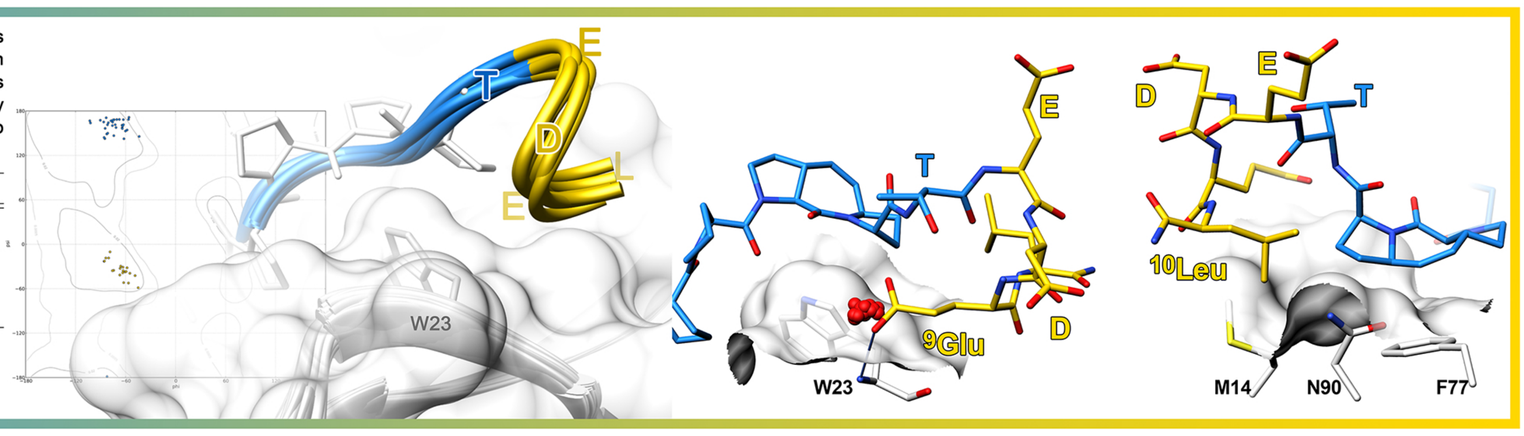

Accessing the additional interaction sites

The polar interaction between Glu and W23 was mimicked in the most simplistic way by the *in silico* designed ProM-12. The unpatented scaffold was incorporated in two inhibitor variations (**5a**, **5c**) which both lost affinity dramatically. The crystal structures of both inhibitors revealed that the ProM-12 scaffolds are lifted off the epitope to minimize steric clashes with the W23 sidechain (PDB codes 5NCP and 5NDU, high resolution cutoffs of 1.65 and 1.42 Å).

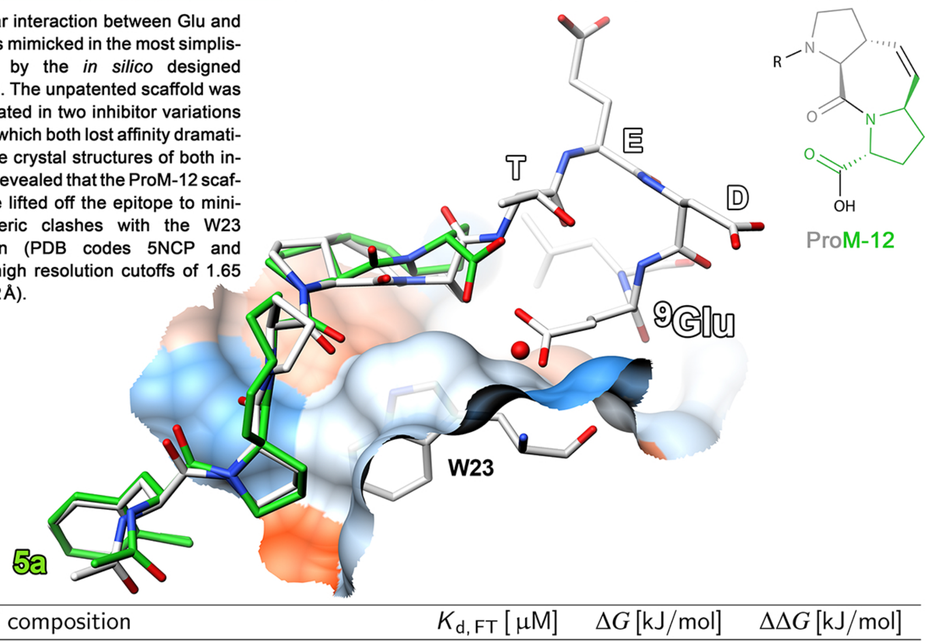

Ligand composition		$K_{d,FT}$ [μM]	ΔG [kJ/mol]	$\Delta\Delta G$ [kJ/mol]
2a	Ac–[2-Cl-Phe][ProM-2][ProM-1]–OH	2.3 (0.2)	–32.2 (0.2)	(ref)
5a	Ac–[2-Cl-Phe][ProM-2][ProM-12]–OH	13.5 (0.4)	–27.8 (0.1)	+4.4 (0.2)
2c	Ac–[2-Cl-Phe][ProM-2][ProM-1]–OMe	4.4 (0.7)	–30.6 (0.4)	(ref)
5c	Ac–[2-Cl-Phe][ProM-2][ProM-12]–OMe	15 (1)	–27.6 (0.2)	+3.0 (0.4)

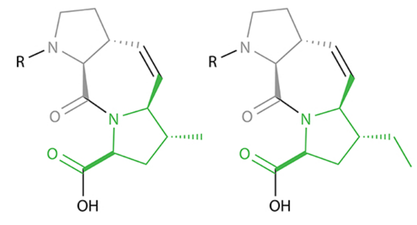

In silico docking studies suggested that the hydrophobic interaction of ProM-1 was increased by enantioselective alkylation (ProM-9 and ProM-13). Both scaffolds outperformed ProM-1 substantially. Inhibitor **7b** regained the entire binding energy of eight flanking amino acids of **2** and increased the molecular weight by 1%, yielding in a potent 734 Da inhibitor. Complex structures with ENAH EVH1 were determined at 1.0 and 1.63 Å resolution (PDB codes 5NCG and 5NBX).

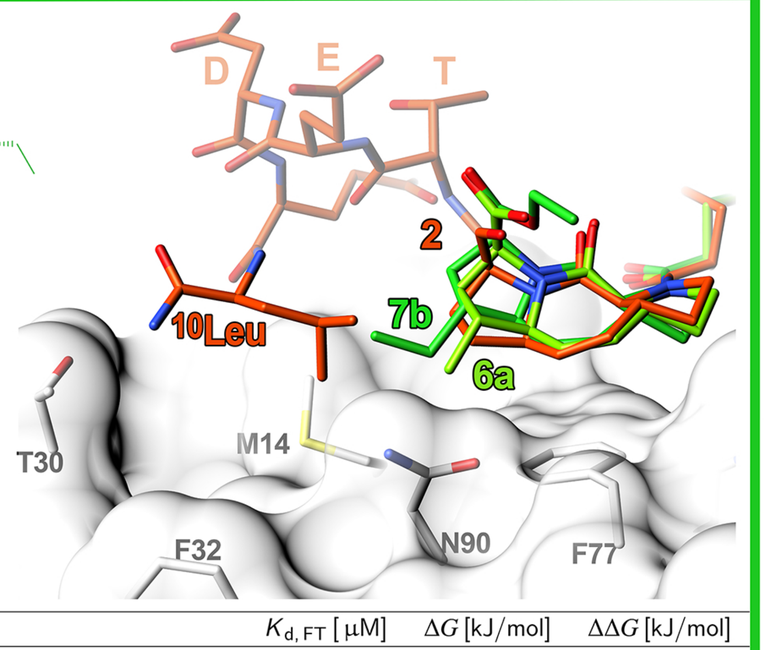

Ligand composition		$K_{d,FT}$ [μM]	ΔG [kJ/mol]	$\Delta\Delta G$ [kJ/mol]
2b	Ac–[2-Cl-Phe][ProM-2][ProM-1]–OEt	4.1 (0.3)	–30.8 (0.2)	(ref)
6b	Ac–[2-Cl-Phe][ProM-2][ProM-9]–OEt	0.38 (0.05)	–36.6 (0.3)	–5.8 (0.4)
7b	Ac–[2-Cl-Phe][ProM-2][ProM-13]–OEt	0.18 (0.03)	–38.5 (0.4)	–7.7 (0.4)
2	Ac–SFE[2-Cl-Phe][ProM-2][ProM-1]TEDEL–NH_2	0.15 (0.02)	–38.9 (0.2)	–8.1 (0.3)

Related recent publication

Opitz, Mueller, Reuter, Barone *et al.*, A modular toolkit to inhibit proline-rich motif-mediated protein-protein interactions, **PNAS** (2015)